# Simulation and Reconstruction of the RICH Upgrade Test Beam

Michele Blago*

**Abstract**
The particle identification using the RICH detector is an essential component of the LHCb experiment. For the upcoming RICH upgrade, which is foreseen for the year 2018, prototypes of the new detector components were tested in a test beam by the RICH upgrade group. A full Geant4 simulation of the set up was created for this purpose. Results obtained from reconstructing the Monte Carlo events were compared with those from the data which was taken during the test beam. This resulted in the measurement of the photon yield and Cherenkov angle resolution.
In order to perform the online monitoring of the test beam and event display program was created.

* Ruprecht-Karls-Universität Heidelberg, blago@physi.uni-heidelberg.de

## Contents



## 1. Introduction

In order to collect data at a rate of 40 MHz at the LHC, components such as new readout chips, photo multiplier tubes (PMT's) as well as the cooling of the system have to be tested for the upcoming upgrade of the RICH detectors in the LHCb experiment. Therefore, a test beam experiment was conducted using the 100GeV beam of the Super Proton Synchroton. The design of the test beam set up is based on previous RICH upgrade test beams, with changes to account for the increased number of hardware components tested.

The computer simulation of the test beam is described. Furthermore, in order to display events of the test beam, an online monitoring program was developed by the RICH upgrade test beam group. The merging of the raw data streams is explained, which is the author's contribution to this online software. The results of the reconstruction of the data taken during the test beam are presented and compared to the results of the Monte Carlo (MC) data which was generated using the simulation. The quantities analysed in this context are the number of photons detected for a single track, the photon yield, as well as the resolution which is obtained for the Cherenkov angle.

## 2. Simulation

### 2.1 Experimental Set Up

The experimental set up is simulated using the Geant4 toolkit. For this purpose, last year's test beam simulation software was used as a starting point and modified. These modifications include major changes in the components itself, changes in the number of components and their positioning as well as their features such as the photon detection efficiency.

#### Radiator Lens

The individual components of the set up can be seen in Figure 1. The purple coloured, spherical object represents the radiator lens. The shape of the radiator is spherical, to which a

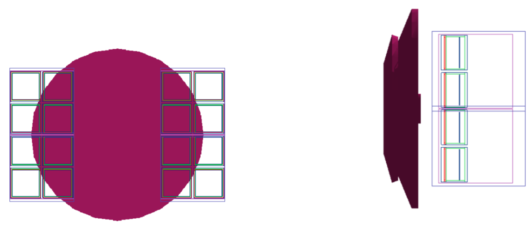

**(a)** Upstream view. **(b)** Side view.

**Figure 1.** Figure 1a illustrates the upstream view on the simulated experimental set up showing the radiator (purple) and elementary cells (squares). Figure 1b shows the side view of the same set up. The beam direction is from left to right. One can see the mirror on the left hand side of the radiator.

short cylinder is added. In this radiator, the Cherenkov photons are emitted from the beam. The radiator substrate is N-BK7 glass which is simulated by including a table of its refractive index as a function of photon wavelength. The information of the mean refractive index is taken from the company that created the lens. Since the refractive index was not measured to check its accuracy it represents a tuneable quantity in order to adapt the Monte Carlo data to the real data results. The refractive index is $n = 1.57$ for photons with a wavelength of $\lambda = 587$ nm. This value is used to adjust the general table of refractive indices. This table does only account for a certain range of wavelengths. Consequently, an uncertainty is introduced in the reconstruction of real and MC data since the refractive index is not constant but varies with wavelength. This uncertainty is discussed in detail in the reconstruction Section 5 and referred to as the *chromatic uncertainty.*

#### Mirror

On the spherical part of the radiator a mirror coating is applied. The reflectivity of the mirror ranges from $\lambda = 200$ nm to $\lambda = 600$ nm which is addressed in the simulation by a table listing reflectivity efficiencies for the individual wavelengths. Photons above or below the range are not reflected in the simulation and only negligibly in the real experiment. In order to selectively reflect the photons originating from the emission point range in which we are interested in, the mirror coating does not cover the whole spherical part of the radiator but rather a circular stripe.

#### Dark Cover

There are two dark covers in the simulation. Their purpose is to absorb photons which would otherwise increase the background noise in the experimental data. Firstly, a dark cover is placed before the radiator lens in upstream direction (upstream dark cover). Here, all the Cherenkov photons which are emitted before the beam enters the radiator are absorbed. Since in the simulation the Cherenkov photons are the only source of photons, this dark cover represents the black box of the real experiment. The black box contains the entire experimental set up and shields hermetically from photons which naturally come from a variety of light sources in the test beam area. Furthermore, the inside of the black box absorbs photons such that there are no reflections from its inside walls producing background noise in the data. An additional feature of the black box in the experimental set up is its insulating property to maintain a stable and cool temperature. These factors are of course not relevant for the ideal world of the simulation. However, they need to be mentioned to stress the differences between simulated and real experiment, which may lead to differences in the results obtained.

The downstream dark cover is a black circular shield that absorbs photons on the flat end of the radiator. By changing the size of this dark cover one can vary the range of Cherenkov photons emitted in the radiator which make it to the PMTs. By allowing more photons to be reflected rather than absorbed on the dark cover one obtains a higher number of photon hits per beam track. However, this decreases also the resolution for the reconstructed Cherenkov angle since the reconstruction assumes that all photons are emitted from the middle point of the whole emission length. This is referred to as the *emission point uncertainty*. The downstream dark cover exists in contrast to the upstream dark cover both in the simulation and the real experiment.

### Elementary Cells

The elementary cells (ECs) are shown as the square objects in Figure 2.

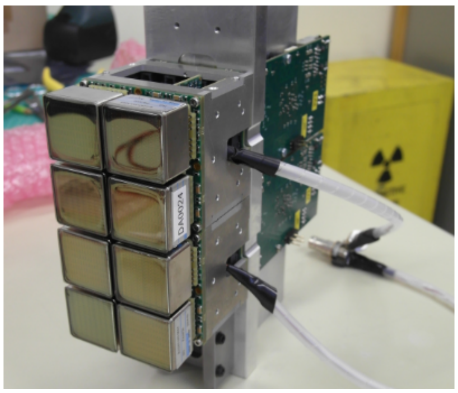

**Figure 2.** Picture of two ECs mounted on top of each other, each holding four PMTs, which can be seen as the small cubical objects.

They contain the PMTs and readout electronics. In this year's set up there are 4 ECs. Each EC can hold up to 4 PMTs. However, only two are placed in each EC in this case. They occupy the positions close to the beam line. When a photon hits the window of one of the PMTs in the simulation, the emission of a photoelectron is calculated using the probability. This is defined in a table, corresponding to its wavelength. This photoelectron is then further simulated with a path parallel to the EC and finally detected, creating a hit point.

The usual path of a Cherenkov photon is shown in Figure 3. It consists of two reflections, one on the flat end of the radiator and one on the mirror, as well as a refraction when exiting the radiator. The generation of a MC event can be seen in Figure 4, again from the upstream perspective (a) and from the side perspective (b), similar to Figure 1. On the left hand side one can see the Cherenkov ring on the PMTs.

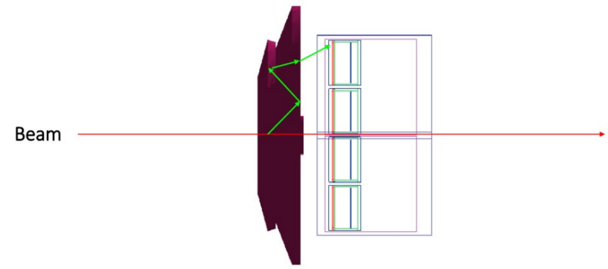


**Figure 3.** The beam direction is shown schematically on the Geant4 simulation as well as the usual path of a Cherenkov photon with two reflections and one refraction.

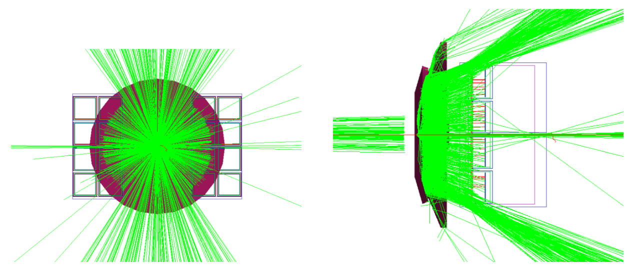

**(a)** Upstream view event. **(b)** Side view event.

**Figure 4.** Analogous to Figure 1 two simulation perspectives are shown, here, in addition an event is displayed.

## 3. Online Monitoring Software

For the first time the RICH upgrade test beam was monitored by a live event display program.

The four elementary cells each produce an individual stream of data. These data streams contain the events originating from two PMTs each. Before this raw data can be processed and translated into hits on a map, the data streams have to be merged into a single one. After this the data are then displayed in a GUI which can be seen in Figure 5a. The author's contribution to the software was to create the program which achieves this merging process.

Since the rate in which data is written to the raw data files is much higher than the rate in which this data can be processed for displaying, event snapshots are shown rather than a live display. This means that in addition to merging the data streams into a single data file, only the

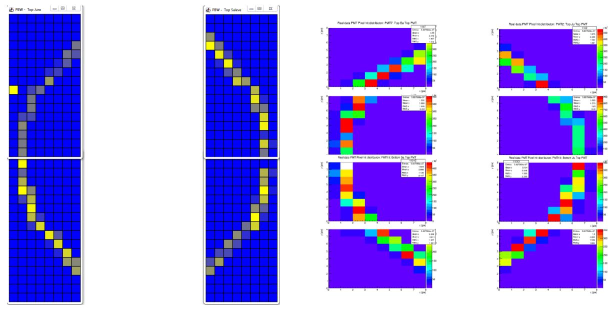

**(a)** Online hit display. **(b)** Data hit display.

**Figure 5.** Figure 5a shows the display output of the online monitoring program. The four sections represent the four elementary cells with two PMT's each. Figure 5b shows the eight histograms for the real hit data of the corresponding PMT's.

last event which is written to the EC raw data files has to be taken for the merging procedure. Meanwhile the order of the data events from the different ECs has to be maintained since this order gives rise to the position of the EC in the experimental set up and hence of the hits which are displayed in the final step.

## 4. Reconstruction

The reconstruction software uses two sources of input. First of all, it requires the hit information: which pixel of a PMT has detected a photon. Secondly, the reconstruction requires information about the set up. This is given by a simulation map which is created from a Monte Carlo sample of events. In this sample the information about the geometrical composition is contained as well as the individual features of the components. Furthermore, the true hit position of the MC events is stored in order to locate typical hit X,Y and Z positions. This is used in the reconstruction since the only information in hit data is the pixel centre position where the hit was detected. The resulting discrete distribution of the hits when using only the hit data is thus transformed to a smooth distribution similarly to the true hit distribution.

#### Photon Yield

The number of photons in each track is described by the photon yield. Figure 5b shows the hit distribution histograms of the real data for the 8 PMTs. One can clearly see the Cherenkov ring which was also obtained in the snapshots of the online monitoring seen in 5a.

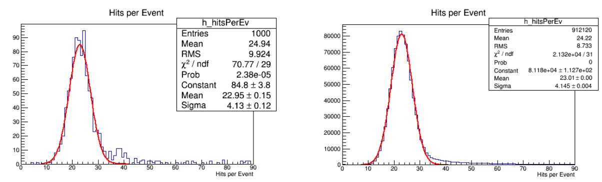


**(a)** Hits per track MC data. **(b)** Hits per track real data.

**Figure 6.** Figure 6a shows the number of photon hits which are detected per track in MC generated data. Figure 6b displays the same result but for the real data. The two distributions peak at the same yield value.

When plotting the number of hits in all the PMTs for each event in a single histogram one obtains the distribution shown in Figure 6. One can see the distribution peaks for the MC data at a value of $n_{photons} = 23 \pm 4$ for both the MC and the real data within the precision of the measurement. One can also see a tail towards higher numbers of photon hits per event. This is discussed in Section 5.

#### Cherenkov Angle Reconstruction

Parameters from the geometry which are used in order to reconstruct the Cherenkov angle from a hit are: the centre of curvature of the mirror, the mirror radius and the photon emission point. For the photon emission point the middle of the range where the photons are created which are not blocked by the downstream dark cover (see Section 2.1) is taken. The hit position, the photon emission point and the centre of curvature of the mirror define the plane on which the true mirror reflection point of the photon has to be located. Therefore, the geometrical intersection of this plane with the mirror sphere gives two solutions for the location of the mirror reflection point, only one of which is the mirror reflection point. One can determine which of the two solutions is the right one since the hit and the mirror reflection point have to be located in the same quadrant when looking at the set up orthogonal to the beam direction. When mirroring the photon emission point on the flat plane of the radiator lens one obtains the so called imaged photon emission point. The angle in which the line between this point and the mirror reflection point intersect with the beam line is the Cherenkov angle under which the photon was originally emitted.

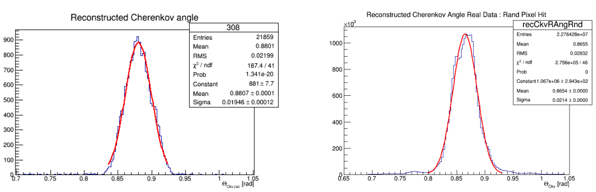


**(a)** Reconstructed Cherenkov angle MC data.

**(b)** Reconstructed Cherenkov angle real data.

**Figure 7.** Figure (a) shows the reconstructed Cherenkov angle for MC generated data, whereas Figure (b) displays the result for the reconstruction of the real data Cherenkov angle. In the latter one can see multiple peaks and a slightly higher mean value.

Figure 7a shows the reconstructed Cherenkov angle for MC real data and Figure 7b the results for the real data. A gaussian fit gives a mean value of $\theta_{MC} = (881 \pm 19)$ mrad for the MC data in Figure 7a. Fitting the real data result one obtains $\theta_{Real} = (866 \pm 21)$ mrad. One can see that the values are matching within their uncertainties even though the real data value is lower than the MC one. Moreover, one can see that the real data distribution shows multiple peaks which will be discussed in Section 5.

## 5. Conclusion

### Photon Yield

The accordance of the two graphs shown in Figure 6 indicates that the simulated experimental set up matches the real set up sufficiently well. The tails towards higher number of photon hits per each event can be explained by secondary particles that arise from the primary beam. These particles can also emit Cherenkov photons which consequently cause a higher number of hits.

### Cherenkov Angle Resolution

The other quantity to measure is the uncertainty with which the Cherenkov angle can be reconstructed. Note that the reconstructed real data value for the angle agrees with the MC one within the error limits. The lower mean value for the real data can be explained by the refractive index of the radiator given in the simulation and reconstruction. Moreover, the real data distribution shows multiple peaks. This is most likely due to the slope of the beam which results in different values for the reconstructed Cherenkov angle for the individual PMTs. The histogram in Figure 7b shows the angle reconstructed for all PMTs together and therefore peaks at multiple positions.

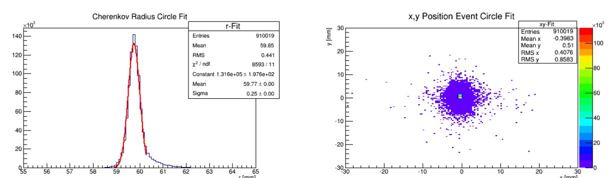


**(a)** Fitted Cherenkov ring radius.

**(b)** Cherenkov circle centre distribution.

**Figure 8.** Figure (a) displays the distribution of Cherenkov ring radii after applying a circle fit to the detected photons. Figure (b) shows the distribution of the circle centre of this fit. One can see a shift of 0.5 mm in x- and y-direction.

One can see the error introduced by the beam slope when applying a circle fit of the hit positions in the real data. The result of this can be seen in Figure 8. Figure 8a shows the radius of the Cherenkov ring which one obtains by the cricle fit. The distribution is fitted by a gaussian. The sharp peak at $R_{Ckv} = (59.8 \pm 0.3)$ mm indicates that the photons are in general well aligned

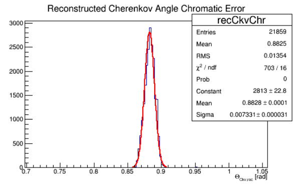


**(a)** Chromatic uncertainty.

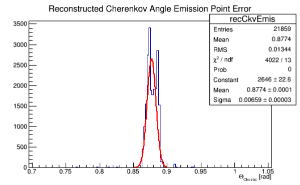


**(b)** Emission point uncertainty.

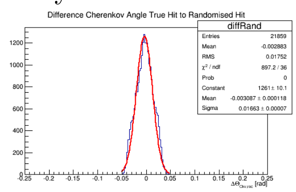


**(c)** Pixel size uncertainty.

**Figure 9.** The different contributors to the total uncertainty in the reconstruction of the Cherenkov angle are shown: the chromatic uncertainty (a), emission point uncertainty (b) and uncertainty due to the finite pixel size (c).

in a circle. A misalignment of the set up from a shift normal to the beam direction has only negligible effects due to the point symmetric shape of the radiator. One can see the shift caused by the beam slope when plotting the centre of the fitted circle as depicted in the histogram in Figure 8b. The mean value is shifted by −0.5 mm in $x$- and $y$-direction.

The beam slope has been measured by the telescope experiment which was also present during the test beam. By using these values as additional information, one can correct for the beam slope in future analyses.

By comparing the MC and real data angle reconstruction results one can conclude that despite their peak position difference the overall reconstruction of the real data shows reasonable results and a similar uncertainty. Consequently, one can use the MC data and its *truth information* to determine the different components which together make up the uncertainty.

When using the real emission point and true detection point the remaining uncertainty is only due to chromatic effects, meaning the error resulting from the approximation of the refractive indices for the different photon wavelengths. This can be seen in Figure 9a with a value of $\sigma_{Chr} = 7.3$ mrad. Analogously one obtains the pixel size uncertainty by subtracting the true hit point reconstructed Cherenkov angle of the from the pixel centre reconstructed angle. This is shown in Figure 9c, resulting in a value of $\sigma_{Pix} = 16.7$ mrad. The error which was introduced by the assumption that the photons are emitted from a single point whereas the true unknown emission point is distributed over a length of $15mm$ is displayed in Figure 9b. The uncertainty of this *emission point error* is $\sigma_{Em} = 6.6$ mrad.

$$\sigma^2_{Calc} = \sigma^2_{Chr} + \sigma^2_{Pix} + \sigma^2_{Em} \quad (1)$$

When summing up the values quadratical as shown in Equation 1, one obtains the same result as the uncertainty of the MC Cherenkov angle reconstruction as displayed in Equation 2.

$$\sigma_{Calc} = 19.4 \text{ mrad} = \sigma_{MC} \quad (2)$$

One can conclude that the uncertainties for the real data are composed in a very similar way. The pixel size is the factor that contributes most to the uncertainty of the reconstructed Cherenkov angle. Consequently, one can improve the resolution by either decreasing the pixel size or by increasing the distance of the PMTs to the radiator lens. The latter would, however, require a larger black box for the whole experimental set up.

## 6. Summary

In this project the RICH upgrade test beam set up has been simulated and reconstructed using Geant4. The results obtained for MC and real data reconstruction are in good accordance and the differences are understood. Furthermore, in this project the data merging for the online display in the RICH test beam has been developed. Both the simulation and reconstruction as well as the online monitoring program are ready to be used for further analysis of this test beam and for future RICH upgrade test beams.